ELSEVIER

Physica B 302–303 (2001) 23–38

PHYSICA B

www.elsevier.com/locate/physb

# DX-like behavior of oxygen in GaN

Christian Wetzel[a,*], Hiroshi Amano[b], Isamu Akasaki[b], Joel W. Ager III[c], Izabella Grzegory[d], Bruno K. Meyer[e]

[a] *High Tech Research Center, Meijo University, 1-501 Shiogamaguchi, Tempaku-ku, Nagoya 468-8502, Japan*
[b] *High Tech Research Center and Department of Electrical and Electronic Engineering, Meijo University, 1-501 Shiogamaguchi, Tempaku-ku, Nagoya 468-8502, Japan*
[c] *Materials Sciences Division, Lawrence Berkeley National Laboratory, Berkeley, CA 94720, USA*
[d] *UNIPRESS High Pressure Research Center, Polish Academy of Sciences, Sokolowska 29/37, 01-142 Warszawa, Poland*
[e] *1. Physikalisches Institut, Justus-Liebig-Universität Giessen, 35392 Giessen, Germany*

**Abstract**

The role of oxygen as a shallow donor and a DX-state in GaN is elucidated by recent Raman experiments under hydrostatic pressure and the findings of first principles calculations. A pressure induced transfer of electrons from a shallow donor state to a deep DX-like state of the same donor can be correlated with vibrational gap modes by monitoring the freeze-out dynamics. Both features are unique to oxygen doped GaN and cannot be observed in Si doped material. The gap modes can be well explained by a linear chain model of impurity vibrations of substitutional O on the N site. A mode variation, and switching steps in its pressure behavior, which occurs in parallel to the carrier freeze-out are proposed to reflect three different charge states of the strongly localized states of O. This DX-type behavior as well as the experimental threshold pressure values are in excellent agreement with the theory results. © 2001 Published by Elsevier Science B.V.

*Keywords:* Gallium nitride; Oxygen; DX-center; Vibrational mode

## 1. Introduction

To classify a solid as a semiconductor requires the capability to control its electrical conduction at will. In this context, however, a wide band gap usually qualifies the crystal as an insulator. A wide band gap semiconductor, therefore, bears the promise to overcome this contradiction to turn an insulator into a semiconductor—by doping. Consequently, introducing shallow electronic level impurities into wide band gap group-III nitrides is the prime challenge for the technological exploitation of this electronic system which is poised to boost efficiency and power density in future optoelectronic and electronic switching applications [1–3]. Donors in GaN play an important role, and we here put into perspective our recent findings on the DX center of the oxygen donor [4–6]. Infrared and Raman spectroscopy with the sample under large hydrostatic pressure are used to monitor the free electron concentration and

*Corresponding author. Tel.: +81-52-832-1151; fax: +81-52-832-1244.
*E-mail address:* wetzel@ieee.org (C. Wetzel).

0921-4526/01/$ - see front matter © 2001 Published by Elsevier Science B.V.
PII: S0921-4526(01)00402-1

characteristic vibrational modes. We compare these results with experimental findings in the literature and with recent first principles theory results [7–12].

The challenge of doping wide-gap materials is well reflected in the properties of group-III nitrides: InN, $E_{gap} = 1.9\,eV$, is usually highly n-type, GaN, 3.4 eV, is typically highly n-type and AlN, 6.2 eV, is typically highly insulating. The technological development of this class of materials to a Billion US-dollar per annum market is directly linked to the ability to control the electronic conduction in GaN for both types, n and p. After the first investigations of as-grown highly n-type GaN in 1969, the challenge to control the free carrier concentration of both types had kept the field at a low rate of research activity as shown in Ref. [1]. Without the ability to reduce n-type conduction to low background levels and to produce p-type material interest in the field gradually declined. It was not until significant improvements in the crystalline quality of GaN using vapor phase epitaxy based on low-temperature deposited buffer layers in 1986 [13] that this trend was inverted and an exponential growth of research and industrial activities was initiated.

The first controlled n-type conductivity by Si doping [14] and successful p-type doping by Mg [15,16] was soon after demonstrated by the same group. The nature of the high donor doping level background limiting the n-type controllability and achievement of p-type conduction, however, was not revealed. The presence of O as an unintentional donor had been suggested [17] but thermodynamical arguments of a very high $N_2$ pressure over the solid favored as a candidate the native defect of the nitrogen vacancy. In fact the nitrogen vacancy became synonymous with the unidentified n-type donor.

When small GaN bulk crystals $(0.3\,mm)^2$ of high crystalline quality [18], became available we devised experiments under large hydrostatic pressure ($p$) to clarify the doping levels and chemical nature of the dopant according to their respective pressure shift. These small platelets had a free electron concentration ($N$) of $1 \times 10^{19}$–$5 \times 10^{19}\,cm^{-3}$ of as-of-then unaccounted origin. In an infrared absorption experiment, Perlin et al. [19] showed that $N$ drops at large hydrostatic pressure of 19 GPa revealing a strongly localized level of the donor with a pressure coefficient smaller than the band gap. In parallel, we showed that the Reststrahlen band in the infrared is restored at 27 GPa demonstrating insulator behavior at that pressure [4]. Also, under these conditions, Raman spectroscopy was used to show that the $A_1$(LO) phonon mode reappears after decoupling from the free carrier plasmon. From a line shape analysis a quantitative interpretation could be performed in terms of $N$ and the level binding energies [4]. Such a behavior was in qualitative agreement with expectations for the native defect of the nitrogen vacancy and not before a study of material with identified donor dopants was it possible to show that such a behavior is that of O [5,20].

This prompts the question of the role of O in the group-III nitrides in general. In compound semiconductors like GaAs and GaP, oxygen induces a deep midgap state, and it does not act as a shallow donor. In fact the discussion of the source of the high n-type background dopant pointed towards Si as the culprit after first principles calculations theory [12] concluded that nitrogen vacancies should be thermodynamically favorable only as a compensating center in p-type GaN. They should not be stable in high densities in n-type material and therefore could not be the very source of $N \gg 10^{16}\,cm^{-3}$. Once, however, the background doping level was reduced, Si-doped GaN shows the typical behavior of a shallow donor with good controllability of $N$ in the range of $10^{17}\,cm^{-3}$–$10^{20}\,cm^{-3}$ [14]. Hall experiments revealed a thermal activation energy of 32 meV [21] in close agreement with the value of effective mass theory. From this it follows that a discussion of the role of O in GaN and the other group-III nitrides would have to be compared with Si.

For this purpose a perturbation experiment under large hydrostatic pressure proved ideally adapted to the problem. Reduction of the lattice parameter under pressure stiffens the lattice potential leading to an energetic shift of Eigenstates. The shift scales with the spatial extension of the wave functions in real space which is the reciprocal of their localization in momentum

space. Electronic states of different localization are therefore classified along their different shift under hydrostatic pressure. In this way effective mass type states will follow the increase of the band gap while states averaging the entire Brillouin zone usually show a much weaker shift [22]. The technique has a second, application-relevant aspect in the simulation of band gap variation by alloying. In the well-studied case of GaAs application of hydrostatic pressure is mutually equivalent to alloying with AlAs into AlGaAs. Results for the binary system under pressure therefore can directly be transferred to the alloy and vice versa.

## 2. Experimental details

The sample material used was small bulk GaN platelets prepared by growth from the solution at large pressure and high temperatures [18]. A SIMS analysis typically revealed an O incorporation of $1 \times 10^{20}\,\mathrm{cm}^{-3}$ [5]. To test a correlation with intentionally doped material, we investigated O doped GaN from hydride vapor phase epitaxy [23] and Si doped material from metal organic vapor phase epitaxy (MOVPE) [21]. As a reference for the phonon spectrum, we used MOVPE material at a low Si doping level of $1 \times 10^{16}\,\mathrm{cm}^{-3}$ [21]. Details of the samples are summarized in Table 1.

Raman spectroscopy in non-resonant excitation by a 100 mW, 476.5 nm beam of an Ar ion laser was performed in $z(-,-)z$ forward scattering geometry of the basal plane. Hydrostatic pressure up to $p = 38\,\mathrm{GPa}$ was applied by means of diamond anvil cells. The pressure medium for all room-temperature experiments was $N_2$. The pressure in the cell was monitored by standard Ruby luminescence and subsequently by the $E_2$ phonon frequency. Infrared reflection was performed using a Fourier transform infrared spectrometer with microscope optics. The dopants electronic donor level is studied by monitoring $N$. Further details are given in the original works [4–6,20].

## 3. DX-type behavior of donor

### 3.1. Free electron concentration in optical spectroscopy

In order to avoid electrical feed-throughs in the pressure cell we rely on contactless optical techniques by means of the interaction of the free carrier plasmon with the LO phonon branch [4]. In forward or backward scattering geometry of wurtzite Raman selection rules allow the observation of $E_2$(low), $E_2$(high) ($=E_2$) and $A_1$(LO) phonon modes [24]. In infrared the $A_1$(TO) mode is active. Consequently it is the $A_1$(LO) mode, or the $E_1$(LO) mode in their respective polarization, that couples to the electric field of the free carrier plasmon.

Fig. 1 presents a series of epitaxial GaN layers on sapphire prepared by MOVPE with variable Si doping concentration in the range from $4 \times 10^{16}$ to $5 \times 10^{19}\,\mathrm{cm}^{-3}$ [25]. As apparent from the selection rules the strong $E_2$ mode is unaffected by $N$ and therefore, serves as a good internal scale for the scattering intensity. In the sample with lowest $N$ the $A_1$(LO) mode appears unperturbed at

Table 1
Parameters of some of the GaN samples studied. $N_D$ denotes the averaged experimental impurity concentration of known donor type species from SIMS profiles. (MOVPE: metal organic vapor phase epitaxy, HVPE: hydride vapor phase epitaxy, HPS: high pressure synthesis, SIMS: secondary ion mass spectroscopy)

| Sample | Growth | $\mu_{el}$ (Hall) ($\mathrm{cm}^2\,\mathrm{Vs}^{-1}$) | $N_{el}$ (Hall) ($10^{16}\,\mathrm{cm}^{-3}$) | $N_D$ (SIMS) ($\mathrm{cm}^2\,\mathrm{Vs}^{-1}$) |
|---|---|---|---|---|
| $O_1$ | HVPE | 90 | 3500 | O: 2000, Si: 30 |
| $O_2$ | HVPE | 124 | 1000 | O: 800, Si: 30 |
| Si | MOVPE | 170 | 1000 | Si:1000 |
| Ref | MOVPE | 410 | 8.9 | Si: 9 |
| Bulk | HPS | 60 | 1000–5000 | O: 10,000, Si: 10 |

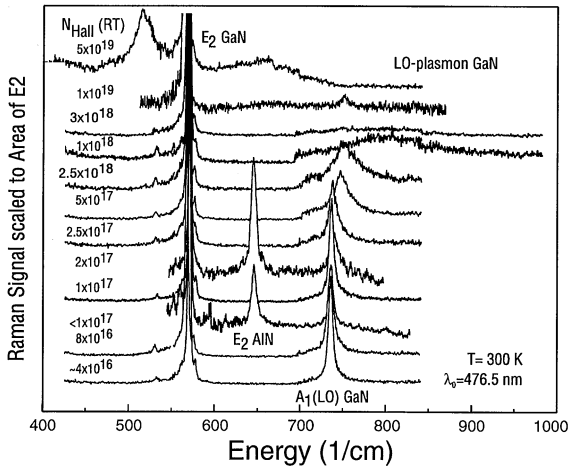


Fig. 1. Raman spectra of the basal plane in GaN layers of different free electron concentration scaled to the $E_2$ peak height. With increasing $N$ the $A_1(LO)$ mode couples with the free electron plasmon and shifts to higher frequencies. After Ref. [25].

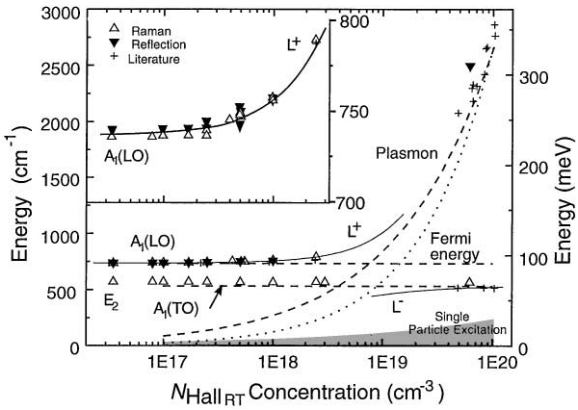


Fig. 2. Experimental (symbols) and theoretical (line) dispersion of the $A_1$ phonon, plasmon, and the $L^-$ and $L^+$ branches of the phonon-plasmon coupled mode. The position of the $L^+$ mode can be used as a direct means to derive the free carrier concentration. After Ref. [25].

$\nu_{max} = 736\,cm^{-1}$. For increasing $N$ the maximum shifts to higher energies, it broadens and its intensity is spread over a wider energy range. This is due to the increased coupling with the free electrons. This range of interaction is seen in Fig. 2, where mode frequencies are plotted versus $N$. The results shown here fall in the $L^+$ coupled range, where the pure phonon-like branch approaches the plasmon branch [26]. The line shape

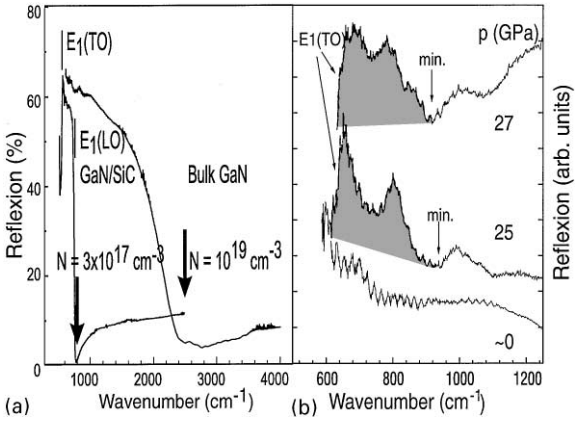


Fig. 3. (a) Infrared reflection of basal plane GaN in the phonon region reveals the Reststrahlen band extending from the $E_1(TO)$ mode to either the $E_1(LO)$ mode for low $N$ or to the phonon-plasmon coupled mode for high $N$. The marked positions of the minima allow a good derivation of $N$. After Ref. [27]. b) The same in highly n-type ($N = 5 \times 10^{19}\,cm^{-3}$) GaN:O as a function of applied pressure. Only at $p = 25$ and 27 GPa the Reststrahlen band appears after the electrons have been captured to their deep donor level. After Ref. [4].

can well be described within an oscillator model based on established parameters and the following relation proves useful [4]:

$$N = 1.1 \times 10^{17}\,cm^{-3}(\nu_{max}/cm^{-1} - 736)^{0.764}. \quad (1)$$

This optical phonon–plasmon coupled mode has proven to be a sensitive way to derive $N$ in the relevant range $10^{16}\,cm^{-3} < N < 10^{19}\,cm^{-3}$. The same coupling can be observed in infrared spectroscopy [4]. Within the same $c$-plane sample orientation $E_1$ modes are infrared active. Within the phonon region enhanced reflection from the well-known Reststrahlen band appears between the TO and the LO phonon frequencies. Here the coupling results in a shift of the reflection minimum on the high energy side of the Reststrahlenband towards higher frequencies and a gradual vanishing of the minimum with increasing $N$. Fig. 3a compares the infrared reflection of a bulk sample with $N = 1 \times 10^{19}\,cm^{-3}$ with that of an epitaxial layer at $N = 3 \times 10^{17}\,cm^{-3}$ grown by the sublimation sandwich method [27]. Again an analysis of the line shape and the position of the minimum of the phonon–plasmon coupled mode within the oscil-

lator model provide good means for a derivation of $N$.

### 3.2. Optical phonons under hydrostatic pressure

Early Raman spectroscopy of GaN under hydrostatic pressure has been performed by Perlin et al. [28]. The $A_1$(LO) mode, however, was not observed. We therefore studied epitaxial GaN with low $N$ up to $p = 25$ GPa and find that $A_1$(LO) scales to higher energies at the same rate as $E_2$ (Fig. 4) [20]. Throughout the $p$-range the intensity ratio of $E_2$ and $A_1$(LO) shows very little variation and $E_2$ also under pressure serves as a reference for the scattering intensity. A constant narrow line width of $E_2$ shows that pressure conditions at the sample have negligible spatial or directional inhomogeneity, e.g., the case of hydrostatic pressure is well supported. After scaling with the Ruby luminescence the linear pressure variation of $E_2$ serves as a secondary pressure standard. These points provide a good set of reference.

### 3.3. Bulk crystals under large hydrostatic pressure

In the next step pressure is applied to the highly n-type bulk crystals while monitoring $N$ by infrared reflection and Raman spectroscopy. Infrared reflection in the phonon region for a highly n-type bulk crystal ($N = 1 \times 10^{19}\,\mathrm{cm}^{-3}$) at ambient pressure and at $p = 25$ and 27 GPa (Fig. 3b) is compared with the signal of the GaN film from sublimation sandwich growth at low $N = 3 \times 10^{17}\,\mathrm{cm}^{-3}$ in Fig. 3a. The Reststrahlen band is clearly resolved at $p \approx 0$ GPa for low $N$, where the plasmon and $E_1$(LO) phonon modes are effectively decoupled. In the case of the highly n-type bulk crystal both are strongly coupled, which essentially wipes out any spectral features. At $p =$ 25 and 27 GPa, however, the Reststrahlen band is restored after decoupling of plasmon and phonon [4]. Considering a pressure shift of the phonons by $+100\,\mathrm{cm}^{-1}$ as derived from the undoped sample we conclude a drop of $N$ to $N < 1 \times 10^{18}\,\mathrm{cm}^{-3}$ revealing the twofold nature of the dominant donor in GaN.

A similar picture can be obtained in the Raman experiment ($A_1$ modes are active, Fig. 5). At ambient pressure no signal can be observed in the $A_1$(LO) range near $\nu = 736\,\mathrm{cm}^{-1}$ due to the strong coupling. Next to $E_2$ a weak set of modes Q

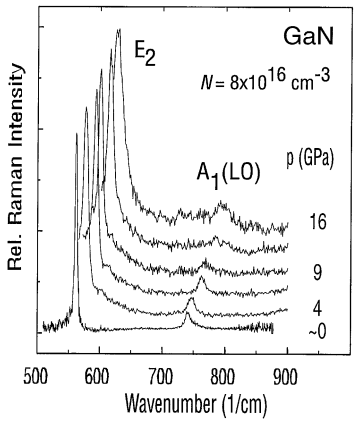


Fig. 4. Phonon spectrum of little doped GaN in Raman spectroscopy as a function of hydrostatic pressure. Both, $E_2$ and $A_1$(LO) shift in proportion to $p$ with little distortion. The behavior of $E_2$ provides a secondary pressure scale and that of $A_1$(LO) serves as a reference. After Ref. [20].

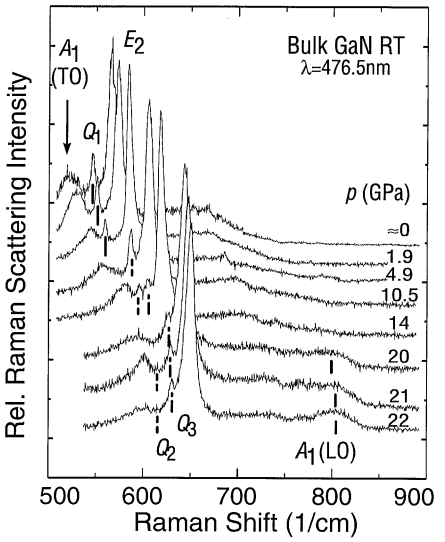


Fig. 5. Raman spectra of the phonon range in highly n-type ($N = 5 \times 10^{19}\,\mathrm{cm}^{-3}$) GaN:O as a function of hydrostatic pressure. Only at $p > 20$ GPa the $A_1$(LO) mode appears after $N$ has dropped to values of $3 \times 10^{17}\,\mathrm{cm}^{-3}$. This reveals the transition from a hydrogenic donor state to a deep level of the same donor. In parallel vibrational modes $Q_1$, $Q_2$, and $Q_3$ appear below $E_2$ with variable intensity and separation from $E_2$. After Ref. [5].

appears that is not part of the known phonon spectrum. For increasing $p$, $E_2$ shifts to higher frequencies. There is little variation in the $A_1(LO)$ phonon range up to $p = 20\,GPa$ beyond which this mode reappears and grows in intensity. The mode set Q, however, observed in parallel shows a shifting to higher energies, with some variation in its separation from $E_2$ and a variation in their respective intensities [6]. Q can be traced back to ambient pressure with a maximum in $v = 544\,cm^{-1}$.

### 3.4. Analysis of the $A_1(LO)$ mode

The reappearance of the $A_1(LO)$ mode near 20 GPa at a frequency expected from its counterpart in the undoped sample reveals that $N$ must have dropped abruptly to values below $3 \times 10^{17}\,cm^{-3}$ as derived from an analysis of its line shape and peak position. In excellent agreement with the observation of the infrared reflection, this data well resolves the abruptness of the transition on this fine $p$ scale. This observation is reversible and the mode vanishes again upon releasing of the pressure. The large dynamics in $N$ and its abruptness shows that there is only one process that produces $1 \times 10^{19}\,cm^{-3}$ carriers. The most likely solution is that the very donor impurities themselves retrap the electrons after switching from a shallow state to a deep one. The pressure induced trapping implies a crossing point of the respective electronic levels on an absolute energy scale.

### 3.5. Model of the pressure dependence of shallow and deep doping levels

Doping of the crystal with isolated atoms implies the orthogonalization of band states of the periodic lattice with the discrete states of individual atoms. In their combination discrete levels of the dopant may so lie in resonance with band states of the host lattice and/or within forbidden band gaps. In the next step the mobile charges rearrange to equilibrate a Fermilevel. In this an occupied state deep in the gap might not be affected. A state in resonance with the conduction band (cb), however, will auto-ionize its electrons to relax to the lower edge of this band. A Coulomb interaction with the doping atom modified by the dielectric constant of the host then binds the electron to the dopant impurity into the well-known effective mass-type hydrogenic states described in turn as a perturbation of the band edge states. For such donors only states in the immediate vicinity of the cb minimum in $\Gamma$ point are needed. These shallow states always co-exist with the higher lying states of the very dopant atom. The perturbation under hydrostatic pressure stiffens the lattice potentials raising electronic levels on an absolute energy scale. Initially the cb shifts much faster than the valence band and the band gap so increases. Besides small variations due to changing effective mass and dielectric constant the shallow donor states directly follow the cb minimum at an initial theoretical pressure rate of $\partial(E(\Gamma_c) - E(\Gamma_v))/\partial p = 37\,meV/GPa$. This is in excellent agreement with the excitonic band gap for $p \leqslant 5.5\,GPa$ (Fig. 6) [29].

A different situation holds for the states associated with the dopant atom. Lacking the periodicity of the lattice due to their localized nature in real space host wave functions of the

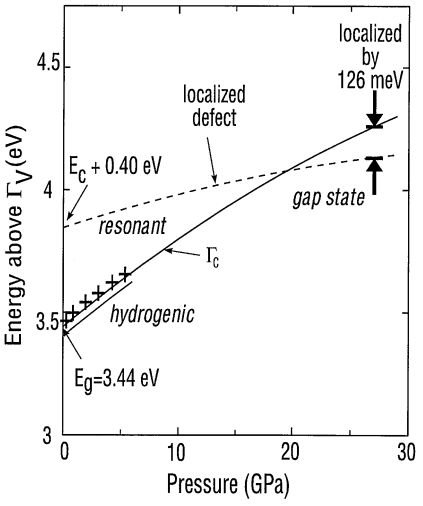


Fig. 6. Bandstructure model of the cb edge and a level averaging the entire Brillouin zone as a function of $p$. Both levels are aligned at 27 GPa to reflect an effective ionization energy of 126 meV derived form the freeze-out dynamics. Both levels cross near 19 GPa and the localized defect level extrapolates to a resonant state at $p \approx 0$. Crosses mark the experimental band gap energy. After Ref. [4].

entire Brillouin zone are required for their representation. An appropriate average of all those states behaves significantly different from the minimum in Γ. On the basis of self-consistent linear muffin-tin-orbital calculations of the electronic band structure in GaN under hydrostatic pressure [30] we developed a model for shallow effective mass states following Γ and strongly localized states averaging the entire Brillouin zone as a function of $p$ [4].

For the localized state we average the $p$-dependent shifts of the points $c \in \{\Gamma, K, M, A, L, H\}$ using a normalized weight function $d_i$. In $d_i$ we include the degeneracy and the number of equivalent points and their direction dependent effective mass according to the given bandstructure calculation [30]. We find $d = 7.1\%$ (Γ), 19% (K), 38% (M), 8.7% (A), 19% (L), and 7.9% (H). The dominance of the M-point results from the slowly varying dispersion in the vicinity of M, which corresponds to a high density of states (DOS). Using these relative weights we obtain the $p$-dependence:

$$\Delta E_{\mathrm{avg}}(p) = \sum_{i=c} d_i[E_i(p) - E_i(0)] = 15.4\,\mathrm{meV}\times p/\mathrm{GPa} - 0.17\,\mathrm{meV}\times(p/\mathrm{GPa})^2. \quad (2)$$

Eq. (2) describes the localized donor state and shows a small upward shift (dashed line in Fig. 6). A recent analysis of the authors of the theory essentially confirms our findings [31]. The drop of $N$ from $1\times10^{19}$ to $3\times10^{17}\,\mathrm{cm}^{-3}$ at 27 GPa requires a binding energy of a single degenerate donor of some 126 meV. We use this value with respect to the cb edge to determine the absolute energy of the localized level (labeled *gap state*).

In fact this neutral donor level crosses the cb edge near 19 GPa in good agreement with the infrared transmission experiments [19]. It extrapolates back to ambient pressure at $E(\Gamma_c)+(0.40\pm0.10)\,\mathrm{eV}$ (labeled *resonant* state). In this range it corresponds to the defect-induced donor level prior to autoionization. A significant drop in electron mobility must be expected once the Fermi energy reaches this level for $N = 1.3\times10^{20}\,\mathrm{cm}^{-3}$. Hsu et al. [32] have considered this case in the AlGaN alloy.

## 4. Identification of the donor

### 4.1. Chemical nature of the defect

To identify the chemical nature of this donor we studied samples with various dopants. Epitaxial HVPE GaN with O doping at $3\times10^{18}\,\mathrm{cm}^{-3}$ and epitaxial MOVPE GaN with Si doping of $1\times10^{19}\,\mathrm{cm}^{-3}$ were compared with the bulk crystals described above. Both are highly doped and coupling to the plasmon prevents the observation of the $A_1$(LO) phonon at ambient pressure. Again, raising the pressure the $A_1$(LO) mode appears for $p > 20$ GPa in the O doped sample. In contrast the $A_1$(LO) mode does not appear in the Si doped material up to the highest applied pressure of 25 GPa [20].

The relative intensities of the $A_1$(LO) mode scaled to that of $E_2$ are shown in Fig. 7 versus $p$ for all the samples. The undoped sample provides the reference for an uncoupled $A_1$(LO) mode. The bulk crystals show vanishing signal for low pressure and a distinct onset for $p > 20$ GPa. The O doped samples show an identical behavior, while the Si doped case shows only little variation. From this correlation we assign the on-set near 20 GPa to a property of the O donor. Beyond $p = 20$ GPa the localized states of O retrap the electrons that thermalize to the cb edge at lower $p$. In contrast Si behaves like a hydrogenic effective mass-type donor within the entire pressure range. Its associated localized level therefore lies at higher energy.

### 4.2. Analysis of gap modes

The observation of the Q-modes beneath the $E_2$ phonon in the bulk crystal deserves special attention [6]. Again we compare this behavior with that of the O and Si doped layers. Fig. 8a shows the respective range in the HVPE GaN:O sample. For comparison the spectra at various $p$-points are aligned at $E_2$. Also in this case the multitude of modes appears with variable intensity

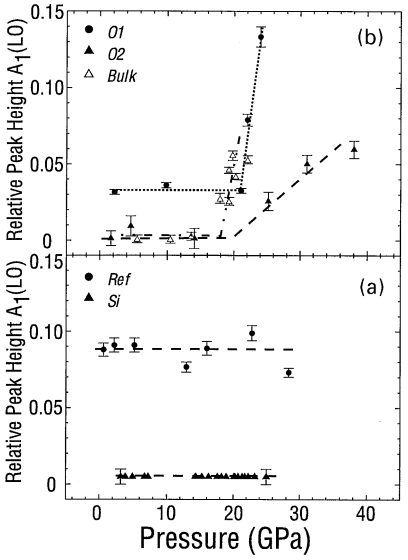


Fig. 7. Relative intensities of the GaN Raman signal in the range of the $A_1$(LO) phonon as a function of $p$ in samples with various doping concentrations and dopants species. The little doped reference sample *Ref* marks a constant level for the insulating case. (a) The highly Si doped sample shows no signal up to 25 GPa revealing that Si remains a shallow donor up to this pressure. (b) Several O doped samples as well as the bulk crystal reveal a characteristic onset at $p = 20 \pm 2$ GPa. This marks a transition from a shallow donor state to a deep gap state. The correlation with O and the large carrier dynamics are evidence of a DX-like center of this very donor. After Ref. [5].

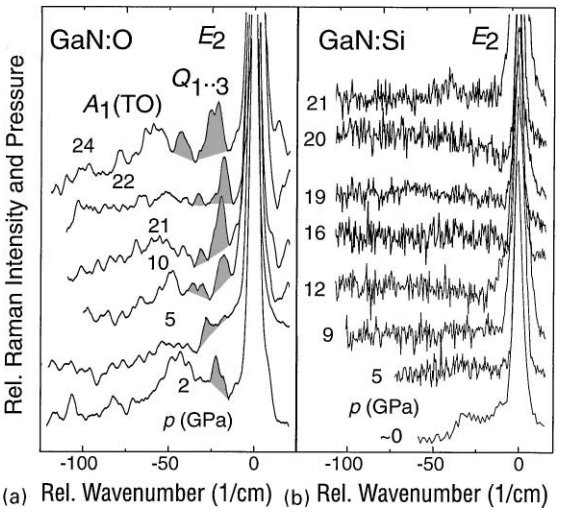


Fig. 8. Vibrational modes $Q_1 \ldots Q_3$ in (a) a highly O doped and (b) a highly Si doped GaN sample as a function of pressure. All spectra are aligned at the $E_2$ center frequency. Several modes can be identified in the O doped case with variable intensity and separation from $E_2$. A complete picture evolves from the analysis of five samples. In the Si doped material no signal can be identified with any similarity to the Q-modes.

and a relative mode shifting towards lower energies. The case of the Si doped material is shown in Fig. 8b. Here no signal whatsoever can be assigned to such a mode and we therefore relate the appearance of the Q-modes to the presence of O. Fig. 9a collects the peak positions of the modes in bulk and O doped samples. Between the $E_2$ phonon modes (straight line) and the $A_1$(TO) phonon we identify a set of three parallel and equidistant modes $Q_1$, $Q_2$, and $Q_3$. With pressure they follow the mode stiffening of $E_2$ but at a smaller rate. The respective intensities scaled to $E_2$ are shown in Fig. 9b. On the basis of the full sample set we observe that mode $Q_1$ dominates in intensity for $p < 11$ GPa, while $Q_2$ is dominant for $11 < p < 17$ GPa. Beyond that $Q_3$ remains the strongest mode. This can be described by an effective mode switching in the sequence of $Q_1$ to $Q_2$ and then to $Q_3$ for increasing $p$. A further step could not be observed up to the highest pressure applied of 38 GPa.

### 4.3. Model of O vibrational gap mode

The phonon dispersion in GaN has been calculated from first principles [33,34]. For the purpose of impurity studies, however, a linear chain of springs and masses has proven to be a suitable and descriptive model [35]. We here consider the hexagonal basal plane of wurtzite GaN [36] and treat three bonds of the bonding tetrahedron as co-planar leading to a regular hexagonal mesh of co-planar lattice sites. A linear chain can be defined along any high symmetry axis with alternating masses of $^{69}$Ga, $m_{Ga} = 69$ amu, and $^{14}$N, $m_N = 14$ amu. To account for the alternating bonding angles we introduce two effective constants $k_1$ and $k_2$ ($k_1 > k_2$) of Hooke springs connecting adjacent nuclei. Imposing a superlattice on the Ga–N chain by such alternating spring constants induces an additional zone folding in reciprocal space. Consequently Eigenvalues of $\Gamma$-modes are proportional to $m_{Ga}^{-1/2}$,

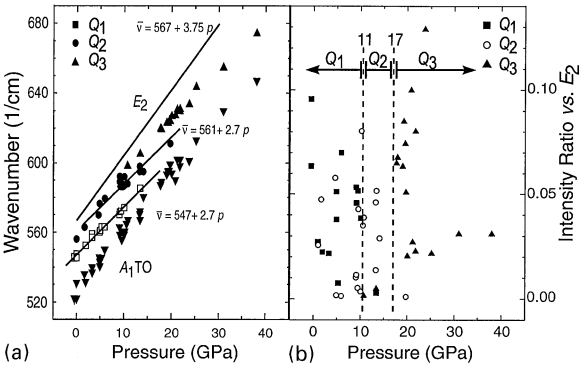


Fig. 9. (a) Mode frequencies of various O doped samples as a function of pressure. $E_2$ appears as a straight line due to its usage as a pressure scale. Between $A_1$(TO) and $E_2$ three bands can be identified with $Q_1$, $Q_2$ and $Q_3$. Their respective pressure coefficients are below that of the phonons. A relative localization energy is derived by scaling to the $E_2$ phonon frequency and taking the difference to the $E_1$(TO) mode which forms the lower edge of the optical phonon branch in this polarization. After Ref. [36]. (b) Relative intensities of the Q modes with respect to that of $E_2$ for the O doped samples. Q dominates for $p < 11$ GPa. $Q_2$ is the strongest for $11 < p < 17$ GPa. For higher pressures up to the highest measured $p = 38$ GPa $Q_3$ dominates. This reveals a respective mode switching from $Q_1$ to $Q_2$ and then $Q_3$. After Ref. [6].

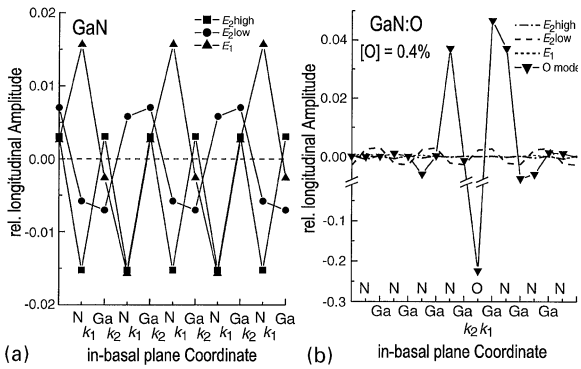


Fig. 10. (a). Longitudinal amplitude distribution of the undoped lattice. Three zone center modes $E_1$, $E_2$(low) and $E_2$(high) are identified. Both force constants are determined by the frequencies of $E_2$(low) and $E_2$(high). $E_1$ then is predicted near the experimental value of the $E_1$(TO) phonon supporting the suitability of the model. After Ref. [36]. (b) Modal amplitudes in the vicinity of O on N site represented by a mass-16 atom on mass-14 site. The vibration is localized to within the first neighbors. The amplitude of O is over tenfold that of the unperturbed $E_2$(high) mode and over 240-fold over that of the perturbed one. This large ratio makes it possible to observe the gap mode experimentally. After Ref. [36].

$m_N^{-1/2}$, and $(1/m_{Ga} + 1/m_N)^{1/2}$, which can be identified as the $E_2$(low), $E_1$, and $E_2$(high) phonons. The splitting of longitudinal and transverse phonons is not accounted here. The respective longitudinal vibration modes are depicted in Fig. 10a. The two parameters of the system, $k_1$ and $k_2$, were adjusted to reproduce the two energies of $E_2$(low) ($\nu = 144\,\mathrm{cm}^{-1}$) and $E_2$(high) ($\nu = 570\,\mathrm{cm}^{-1}$). As a test a third value for $E_1$, ($\nu = 555\,\mathrm{cm}^{-1}$), was derived which closely coincides with the experimental $E_1$(TO) mode and confirms the suitability of the model. The large ratio of $m_{Ga}/m_N$ leads to a narrow optical phonon band and a large splitting of acoustical and optical phonon branches.

The role of O impurities on the N-site is studied in the same model by replacing one mass of 14 amu by the mass of 16 amu. This constitutes the case of isoelectronic doping, where the additional charge of O is neglected. The modified phonon modes and the O impurity mode are shown in Fig. 10b. The O mode is limited to the two nearest neighbors on either side and resembles that of $E_2$(high). In the larger vicinity of the impurity the amplitudes $\hat{e}$ and consequently the transition probability $\propto \hat{e}^2$ of $E_2$(high) and $E_1$ phonons are strongly reduced. In turn the amplitude of the O atom is very strong and leads to a $(\hat{e}_O/\hat{e}_{E2})^2 \approx 220$-fold increased transition probability with respect to the $E_2$(high) mode in the unperturbed system. The increase then is even higher $\approx 20\,000$-fold in relation to the damped $E_2$ mode in the perturbed case. For a linear chain of 256 atoms the phonon dispersion including the one $O_N$ impurity equivalent to a 0.4 at% doping concentration was calculated leading to the DOS in Fig. 11. The O mode appears as gap mode at $532\,\mathrm{cm}^{-1}$ below the optical phonon band extending from $E_1$ to $E_2$. Despite the small fraction of the O-related mode in the phonon DOS, because of its large oscillation amplitude it may be well observed in experiment. This calculated value is very close to the values of the Q mode at ambient pressure $\nu = 544\,\mathrm{cm}^{-1}$ and

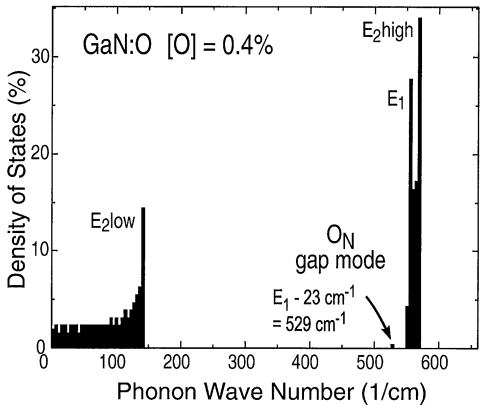


Fig. 11. Density of basal plane vibrational modes in the linear chain model of wurtzite. A gap mode of O on N site appears at $529\,cm^{-1}$ in perturbation to the optical phonon branch with a binding energy of $23\,cm^{-1}$. Due to its strong expected amplitude this mode should be observed in a Raman experiment. After Ref. [36].

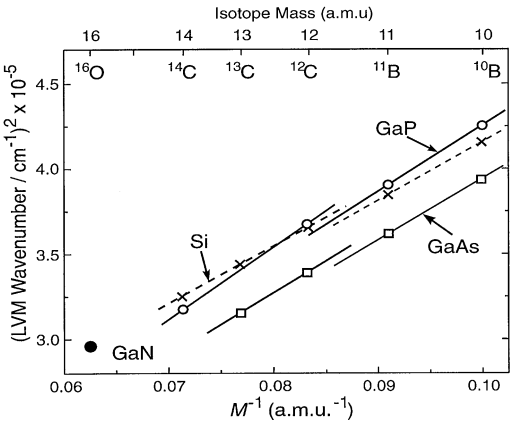


Fig. 12. Vibrational modes of light substitutional impurities in Si, GaAs and GaP after Newman [37]. Within the model of an isolated oscillator the square of the mode frequency is proportional to the isotope mass. Our experimental value of Q is in excellent extrapolation of the GaP modes of $^{10}B$, $^{11}B$, $^{12}C$, $^{13}C$, and $^{14}C$.

strongly supports a possible nature of the Q modes in vibrational gap modes below and in perturbation to the optical phonon branch.

Within an independent model Newman et al. [37] found a good linear approximation of the square of the impurity mode frequency to the isotopic mass of the impurity for light dopants on the group-V site in GaAs and GaP. Both models merge under the assumption of the Ga mass approaching infinity. In this case the problem of a chain of two different masses reduces to a single particle problem of a single light element (Born approximation). The single particle model qualifies as a good approximation due to the strong localization of the O vibration to only one neighboring cell. Fig. 12 depicts the extrapolation of that model over the light group-V lattice site substitutions towards $GaN:O_N$. The value of Q at ambient pressure $\nu = 544\,cm^{-1}$ falls within 8% of the extrapolated value.

Recently Fall et al. [38] approached the problem of the O vibrational gap mode in GaN in a first principles calculation. According to their results a strong $O_N$ associated gap mode should appear near $500\,cm^{-1}$ in infrared absorption which is again in good agreement with our experimental modes in Q.

### 4.4. Mode variation and switching

After this assignment of Q to the gap mode of substitutional O on the N site of GaN we shall discuss the pressure induced variations and switching of these modes. We therefore consider a Coulombic charge of the defect. Small variations of the force constants in the linear chain model are introduced by a scaling factor $\kappa$ to the pair of $k_1$ and $k_2$ next to the impurity atom. Theoretical frequencies in dependence of $\kappa$ are shown in Fig. 13 together with the experimental threshold localization levels A, B, and C. The case of decoupled oscillators ($m_{Ga} \to \infty$) is also shown (solid line). Within the model of coupled oscillators (filled squares), the switching sequence of the $Q_1 \ldots Q_3$ modes appears as follows. Starting at level B ($\kappa = 1.05$), Q moves to C and $\kappa$ falls to $\kappa = 1.00$ before with increasing $p$ it switches back to B and $\kappa = 1.05$. It then moves up again towards C. In Modes $Q_2$ and $Q_3$ coexist with the dominant mode. They first appear at or near level A ($\kappa = 1.11$) and move to B and C before they receive the major intensity, respectively. This variation of 5% in the force constants compares reasonable with the relative change of the nucleus charge from N to O (14%) and the calculated

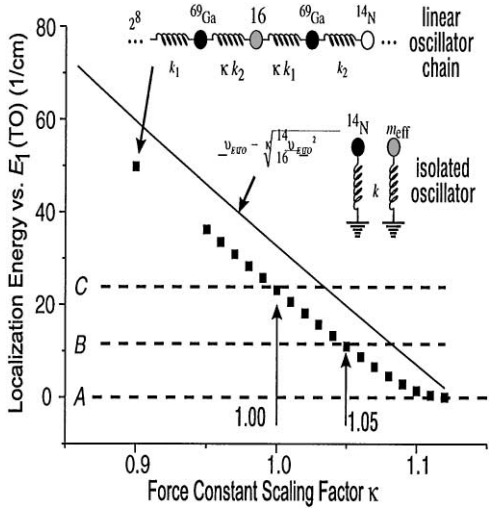


Fig. 13. Variation of the linear chain model to include for Coulombic charge on the mass-16 dopant by scaling the neighboring force constants with *eq*. A linear variation of the binding energy of the vibration mode is found in the model of isolated oscillators. Including coupling in the linear chain a retarded response is seen. A variation of *eq* by 5% around the isoelectronic case of $eq = 1.00$ can explain the experimental shifts and steps in the Q-modes. After Ref. [6].

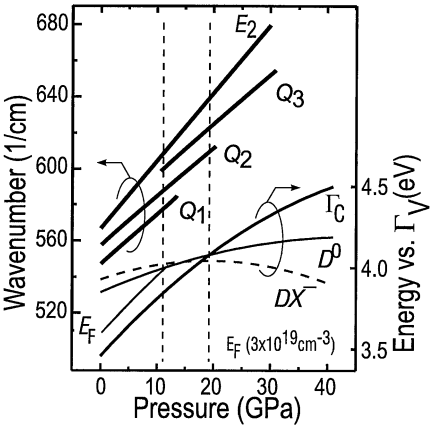


Fig. 14. Correlation of experimental Q mode variations with pressure and the level scheme of the electron trapping to the deep center of O. Three Q modes reveal three different charge states with transition pressures near 11 and 17 GPa. The latter corresponds to the transfer of electrons to the deep gap state. The threshold at 11 GPa falls close to the expected merging of the neutral defect level with the Fermi edge for $N = 3 \times 10^{19}\,\mathrm{cm}^{-3}$. We therefore propose a sequence of the atomic charge states from $D^+$ ($p < 11$ GPa) to $D^0$ ($11 < p < 17$ GPa) and $D^-$ ($p > 17$ GPa). This close correlation with the freeze-out dynamics of the O DX-center therefore suggests a nature of the Q mode in the vibrational gap mode of O on N-site in GaN. After Ref. [36].

bond length variation of 3–4.2% around the O impurity in GaN [9,10]. Within this limited model the continuous variation of the localization energy results from changing screening conditions of the defect as defect level and Fermi level approach each other for changing $N$. The discrete steps from $Q_1$ to $Q_2$ and $Q_2$ to $Q_3$ corresponding to $\Delta\kappa \approx 0.05$ in turn are explained as transitions between the different charge states of that defect. Such a variation of the vibrational mode energy with the charge state has also been seen for Si in InP [39].

It is an important observation that the switching threshold from $Q_2$ to $Q_3$ closely coincides with the pressure threshold for the appearance of the $A_1$(LO) mode within the very same experiment. This points to the question of the role of the first threshold at $p = 11$ GPa. An answer can be found (Fig. 14) when we include the Fermi-edge ($N = 3 \times 10^{19}\,\mathrm{cm}^{-3}$) as a function of $p$. A threshold of $p = 11$ GPa marks the crossing of the Fermi edge with the neutral localized donor level. For $p > 17$ GPa the Fermi-edge then is determined by the strongly localized level.

Therefore, the close correlation of both threshold levels with characteristic events of the carrier freeze-out to the strongly localized level of O represents a direct monitoring of its very charge state. The threshold nature of the Q-modes reveals three different configurations involved during the pressure induced trapping process. A neutral charge state follows for 11 GPa $< p <$ 17 GPa where the Fermi energy coincides with the neutral level. A positive charge state follows for $p < 11$ GPa, where carriers auto-ionize to the cb edge. For $N$ below the Mott transition carriers then bind to the shallow effective mass donor states. Also in the limit of low $N$ both pressure thresholds would merge near the higher one for a decreasing Fermi energy. An additional configuration of the defect then follows for $p > 17$ GPa. In the sequence of positive and neutral states this third one must be

negative in charge. The sequence of charge states is also supported by the constant step size of switching from $Q_1$ to $Q_2$ and to $Q_3$ (Fig. 9b). This implies that O should act as a net acceptor for the highest pressures compensating other possible donors such as Si. This close monitoring of the freeze-out dynamics to the O donor level by the Q-modes is strong evidence for a nature of Q in vibrational gap modes of O in GaN.

### 4.5. Oxygen as a shallow donor

The shallow donor nature of O in GaN at ambient pressure has also been disputed in the literature. In early photoluminescence studies a frequently observed luminescence band a 3.42 eV at 4 K was correlated with O doping [40]. Also in AlN deep luminescence bands have been associated with deep gap states of O. In electron irradiated GaN Chen et al. [41] find a detail-rich set of luminescence lines in the infrared and characteristic phonon replica that resemble those in GaP : O, which had been attributed to internal transitions of deep midgap states of O. Indeed O does not induce a shallow donor state in GaP. This similarity suggests that such deep levels of O also exist in electron irradiated GaN : O. This questions the existence of a shallow donor state and the role of the electron irradiation needed to observe that luminescence band. A recent first principles theory study [38] proposes here the involvement of O complexes, a model that could not be excluded in the case of GaP. A direct scaling and good quantitative agreement of $N$ as determined by Hall transport experiments with the O incorporation determined by SIMS depth profiles over a wide concentration range by Meyer et al. [42] recently, however, unambiguously establishes that there is a shallow O donor level in as-grown GaN material. The presence of further deep midgap levels or complexes associated with O cannot be ruled out from these observations.

### 4.6. DX-like center of O in GaN

The combination of both observations in a single experiment, transfer of the O induced high electron charge density to a deep donor level of O and a vibrational gap mode that tracks the individual charge steps of the electron trapping process are strong evidence for a carrier capture process to a strongly localized state of O. The fact that three different charge states are distinguished requires that O is in the negative charge state for $p > 20$ GPa. Such a situation is typically the case for DX centers well-studied in other III–V compounds. In that case the trapping of the second electron is accompanied by a large lattice relaxation of either the impurity or its environment. Direct evidence for such a relaxation was not yet identified by our experiments. The gap vibrational mode considered here is limited to a vibration within the basal plane of the uniaxial wurtzite structure. A relaxation out of this plane along the $c$-axis may not reveal in the in-plane vibration frequency.

### 4.7. Transfer of results to AlGaN

The application of pressure to GaN has a direct and technologically relevant analog in the alloying of GaN to form AlGaN. The increase of the band gap with either pressure or alloy composition can be used as the common scaling parameter. According to the bandstructure model in Fig. 6 the crossing point of the cb edge and the strongly localized level occurs at a band gap energy of 4.08 eV. The corresponding AlN fraction in $Al_xGa_{1-x}N$ is $x = 0.40$. We therefore expect that O induces a shallow effective mass level in AlGaN only for $x < 0.40$. For $x > 0.40$ we conclude a negatively charged deep gap state. O can therefore not act as a donor for higher $x$ and it furthermore should act as a compensating acceptor for carriers induced by other, shallow donors. On the contrary, the localized level of Si could not be found in the pressure experiment up to $p = 25$ GPa or a band gap energy of 4.22 eV. This transfers to an AlN fraction of $x = 0.56$. Up to this composition we expect Si to behave as a shallow effective mass-type donor in AlGaN. The range of higher $x$ is beyond the results of our experiments.

Early experiments on the conductivity in AlGaN versus $x$ [43] find a transition to an insulator behavior for $x$ approaching $x = 0.3$. This can now be interpreted as the presence of O as the

dominant donor species. In a very recent photoconductivity study in $Al_xGa_{1-x}N$ for various $x$ McCluskey et al. [44] find persistent conductivity with increasing trapping barrier for increasing $x$. The barrier extrapolates to a crossing point of deep level and cb edge at $x = 0.3$ in reasonable agreement with our extrapolation of the pressure experiment. This observation was specific to samples incorporating O. Si doped material in turn did not show this effect up to $x = 0.44$. This activation barrier is another evidence for a strong lattice relaxation typical for DX centers and supports our assignment to a DX-like behavior of O in GaN.

Experiments by Suski et al. [45] cycling Si doped $Al_xGa_{1-x}N$ ($0.5 < x < 0.6$) in pressure and temperature show that also such material exhibits persistent conductivity. This shows that either also Si induces a deep gap (DX) state for $x > 0.5$ or that traces of O in the deep gap state can compensate the shallow Si donor. The fact that highly conducting AlGaN layers can be obtained in MOVPE by Si doping up to $x = 0.79$ on sapphire [46] and up to $x = 0.5$ on AlN [47], however, shows that Si is a shallow donor up to very high AlN fractions.

AlN is typically highly insulating and it is of significant scientific and technological interest to achieve an n-type conductivity. Due to its strong affinity with Al oxygen is a very likely contaminant during the growth. AlN is also strongly subject to oxidation after the growth on the time scale of months. The finding of a deep DX-like level of O in AlGaN therefore can well explain the insulator nature of AlN. However, recently the group of Stutzman et al. [48] have been successful in achieving n-type persistent photoconductivity in Si doped AlN. The fact that such could not be observed in O containing material shows that the Si induced levels are higher in the band gap than the O related.

## 5. Impurity localization in theory

The problem of the O impurity also has attracted strong interest in theory and several groups have studied the problem with first principles calculations. The solubility of impurities in group-III nitrides as well as their role as shallow or strongly localized deep dopants was studied by Boguslawski, Briggs and Bernholc [49,50], Mattila and Nieminen [9], Park and Chadi [10], and Stampfl and Van de Walle [11]. A classification of impurity ground states into shallow and strongly localized states as revealed by large lattice relaxations has been obtained. C, O, S, Si, Ge, Be, and Mg [7] impurities were considered on both substitutional lattice sites. Various configurations for DX-centers are found including a large relaxation of the impurity along the $\langle 0\,0\,0\,1\rangle$ $c$-direction ($DX_1$, or $\gamma$-BB DX configuration) or the $\langle 1\,0\,0\,0\rangle$ $a$-direction ($DX_2$, or $\alpha$-BB DX configuration) (BB: broken bond) [10,50]. Park and Chadi in addition consider a cation–cation bond (CBB) formation of the first impurity neighbors [10]. Differences of the various models include the number of points considered to represent the Brillouin zone and the treatment of the Ga 3d bands as either explicit valence or core states. The calculations also differ in the treatment of wurtzite and zincblende host lattices. Some values are obtained by transfer of the results obtained in one structure, others are obtained by considering the respective structure already in the initialization of the calculations.

On the cation site C, Si and Ge are found to be effective mass type donors in GaN [10,50,51]. Self-compensation and pairing of C, Si and Ge are found to be negligible in $Al_xGa_{1-x}N$ only for $0 < x < 0.4$ under Ga rich conditions [49,50]. In AlN Bernholc and Boguslawski [50] and Park and Chadi [10] find that Si should form a $DX_1$ state. Here Van de Walle [12] finds a positive correlation energy $U = +0.31$ eV and no stable DX center. Consequently transitions between both, a shallow donor nature and a DX center are expected in $Al_xGa_{1-x}N$ in theory for both, Si and Ge. In turn Bernholc and Boguslawski [50] predict Si to transfer into a DX state for $x > 0.6$ while Park and Chadi find a threshold as early as $x > 0.24$ [10].

Van de Walle [12] predicts that Si should not form a DX center in AlN, which is in excellent agreement with our experimental pressure results transferred to AlGaN alloys. This is also in good agreement with the fact that $Al_xGa_{1-x}N$ can be

made n-type by doping with Si up to a concentration of $x = 0.79$ [46] and the demonstrated photoconductivity in Si doped AlN [48].

Next let us consider substitutions on the N site. O is known experimentally [11,17] to incorporate as a donor. From our perturbation by large hydrostatic pressure O is found to behave as a shallow donor for pressure below $20 \pm 2$ GPa [5]. Then as shown O above $20 \pm 2$ GPa behaves as a strongly localized donor exhibiting DX-type behavior. Within the framework of the different approaches theory very well agrees with these findings predicting a shallow donor behavior in GaN under normal conditions [9,10,12]. Van de Walle [12] performed calculations for equilibrium and a reduced crystal volume corresponding to a pressure of 41 GPa and finds a DX behavior with a large relaxation of the O impurity towards the third nearest Ga neighbor for pressures above 18 GPa in excellent agreement with our experimental results. The correlation energy for the $DX^-$-state is found to decrease from $U = +0.48$ eV (ambient pressure) to $U = -0.62$ eV (41 GPa). This pressure result is found exclusively for wurtzite GaN, but not for the zincblende polytype. Park and Chadi calculated a transition pressure of 22 GPa [10].

In AlN Youngman and Harris [52,53] and Pastrnak [54] found O to induce deep gap states experimentally in luminescence. Recent theory indeed finds a DX behavior in wurtzite AlN ($U = -2.5$ eV [10], $-0.57$ eV [12]). Similar to the pressure results Van de Walle predicts this to be unique to the wurtzite phase [12]. Accordingly transitions between shallow donor and DX-behavior are expected in AlGaN. Dependent on the assumed interpolation schemes used by the different groups different critical compositions are found. Based on a linear variation of the bandgap in GaN with pressure and AlGaN with composition we [5] expect O to convert into a deep state at $x = 0.40$ while Van de Walle predicts $x = 0.46$ [12]. Based on a bowing parameter in AlGaN of $b = -0.53$ eV a value of $x = 0.30$ is found derived from the pressure experiments [12]. Mattila and Nieminen [9] as well as Park and Chadi [10] predict a threshold composition as small as $x = 0.2$.

## 6. Conclusion

The role of oxygen in its shallow donor and its DX states in GaN has been put into perspective with recent experimental and theoretical results. In experiments under perturbation of large hydrostatic pressure we have identified a DX-type behavior of O in GaN by its conversion from a shallow donor to a deep doping level. The freeze-out dynamics could be directly monitored by the variation and switching of a vibrational gap mode that most-likely is that of O substituting on the N site. We distinguish three different states of this mode and attribute those to ionized ($DX^+$), neutral ($DX^0$) and double occupied ($DX^-$) charge states of the substitutional O donor. All of those findings are specific to O doped material and within the limits of our investigation no such effect could be observed for the Si donor. All of these results are in excellent qualitative and quantitative agreement with recent results of first principles calculations. The drawn conclusions concerning the roles of O and Si in AlGaN alloys have since been verified independently in experiment and theory. The threat of O contamination during growth and during device lifetime therefore must be given a high priority in group-III nitride technology due to its unusual behavior. In its scientific aspects we have established an important link between the world of semiconductors and insulators in the form of ceramics.

## Acknowledgements

This work was supported in part by the Japan Society for the Promotion of Science "Research for the Future Program in the Area of Atomic Scale Surface and Interface Dynamics" under the project of "Dynamic Process and Control of the Buffer Layer at the Interface in a Highly-Mismatched System (JSPS96P00204)" and the Ministry of Education, Science, Sports and Culture of Japan (Contract Numbers 11450131, 12450017 and 12875006). Work at Berkeley Lab was performed under Cooperative Research and Development Agreement with HP Laboratories and supported by the Director, Office of Sciences of the

US Department of Energy under Contract No. DE-AC03-76SF00098. C.W. thanks the A.C. Bindereif Foundation for a time grant. The authors thank P. Perlin for advice concerning pressure experiments, T. Suski for fruitful discussions, and E.E. Haller and P.Y. Yu for the use of their pressure equipment.

## References

[1] I. Akasaki, in: F.A. Ponce, S.P. DenBaars, B.K. Meyer, S. Nakamura, T. Strite (Eds.), Nitride Semiconductors, Materils Research Society Symposium Proceedings, Vol. 482, 1998, pp. 3–14.
[2] I. Akasaki, C. Wetzel, Proc. IEEE 85 (1997) 1750.
[3] I. Akasaki, H. Amano, in: G.B. Stringfellow, M.G. Craford (Eds.), High Brightness Light Emitting Diodes, Semiconductors and Semimetals, Vol. 48, Academic Press, London, 1997, p. 357.
[4] C. Wetzel, W. Walukiewicz, E.E. Haller, J. Ager III, I. Grzegory, S. Porowski, T. Suski, Phys. Rev. B. 53 (1996) 1322.
[5] C. Wetzel, T. Suski, J.W. Ager III, E.R. Weber, E.E. Haller, S. Fischer, B.K. Meyer, R.J. Molnar, P. Perlin, Phys. Rev. Lett. 78 (1997) 3923.
[6] C. Wetzel, H. Amano, I. Akasaki, J.W. Ager III, I. Grzegory, M. Topf, B.K. Meyer, Phys. Rev. B 61 (2000) 8202.
[7] C. Wetzel, I. Akasaki, in: J. Edgar, T.S. Strite, I. Akasaki, H. Amano, C. Wetzel (Eds.), Properties, Synthesis, Characterization, and Applications of Gallium Nitride and related Semiconductors, INSPEC, IEE, London, UK, 1999, p. 284.
[8] C. Wetzel, T. Suski, J.W. Ager III, W. Walukiewicz, S. Fischer, B.K. Meyer, Proceedings of the 23rd International Conference Physics Semiconductor, World Scientific, Singapore, 1996, p. 2929.
[9] T. Mattila, R.M. Nieminen, Phys. Rev. B 54 (1996) 16676.
[10] C.H. Park, D.J. Chadi, Phys. Rev. B 55 (1997) 12995.
[11] C. Stampfl, C.G. Van de Walle, Appl. Phys. Lett. 72 (1998) 459.
[12] C.G. Van de Walle, Phys. Rev. B. 57 (1998) R2033.
[13] H. Amano, N. Sawaki, I. Akasaki, Y. Toyoda, Appl. Phys. Lett. 48 (1986) 353.
[14] N. Koide, H. Kato, M. Sassa, S. Yamasaki, K. Manabe, M. Hashimoto, H. Amano, K. Hiramatsu, I. Akasaki, J. Crystal Growth 115 (1991) 639.
[15] I. Akasaki, H. Amano, M. Kitoh, K. Hiramatsu, N. Sawaki, Extended Abstract, (175th Spring Meeting) 1989, Electrochem. Soc., Vol. 673, SOA.
[16] H. Amano, M. Kitoh, K. Hiramatsu, I. Akasaki, J. Electrochem. Soc. 137 (1990) 1639.
[17] W. Seifert, R. Franzheld, E. Butter, H. Sobotta, V. Riede, Cryst. Res. Technol. 18 (1983) 383.
[18] I. Grzegory, J. Jun, M. Bockowski, St. Krukowski, M. Wroblewski, B. Lucznik, S. Porowski, J. Phys. Chem. Solids 56 (1995) 639.
[19] P. Perlin, T. Suski, H. Teisseyre, M. Leszczynski, I. Grzegory, J. Jun, S. Porowski, P. Boguslawski, J. Bernholc, J.C. Chervin, A. Polian, T.D. Moustakas, Phys. Rev. Lett. 75 (1995) 296.
[20] C. Wetzel, A.L. Chen, T. Suski, J.W. Ager III, W. Walukiewicz, Phys. Stat. Sol B 198 (1996) 243.
[21] W. Gotz, N.M. Johnson, C. Chen, H. Liu, C. Kuo, W. Imler, Appl. Phys. Lett. 68 (1996) 3144.
[22] D.J. Chadi, K.J. Chang, Phys. Rev. B 39 (1989) 10063.
[23] M. Topf, S. Koynov, S. Fischer, I. Dirnstorfer, W. Kriegseis, W. Burkhardt, B.K. Meyer, Mater. Res. Soc. Proc. 449 (1997) 307.
[24] C.A. Arguello, D.L. Rousseau, S.P.S. Porto, Phys. Rev. 181 (1969) 1351.
[25] C. Wetzel, I. Akasaki, in: J. Edgar, T.S. Strite, I. Akasaki, H. Amano, C. Wetzel (Eds.), Properties, Synthesis, Characterization, and Applications of Gallium Nitride and related Semiconductors, INSPEC, IEE, London, UK, 1999, p. 52.
[26] P. Perlin, J. Camassel, W. Knap, T. Taliercio, J.C. Chervin, T. Suski, I. Grzegory, S. Porowski, Appl. Phys. Lett. 67 (1995) 2524.
[27] C. Wetzel, D. Volm, B.K. Meyer, K. Pressel, S. Nilsson, E.N. Mokhov, P.G. Baranov, Appl. Phys. Lett. 65 (1994) 1033.
[28] P. Perlin, C. Jauberthie-Carillon, J.P. Itie, A. San Miguel, I. Grzegory, A. Polian, Phys. Rev. B 45 (1992) 83.
[29] C. Wetzel, W. Walukiewicz, E.E. Haller, H. Amano, I. Akasaki, in: S. Ashok, J. Chevallier, I. Akasaki, N.M. Johnson, B.L. Sopori (Eds.), Defect, Impurity Engineered Semiconductors and Devices, Proceedings of Materials Research Society Symposium, Vol. 378, 1995, pp. 509–514.
[30] N.E. Christensen, I. Gorczyca, Phys. Rev. B 50 (1994) 4397.
[31] I. Gorczyca, A. Svane, N.E. Svane, Phys. Rev. B 60 (1999) 8147.
[32] L. Hsu, W. Walukiewicz, Phys. Rev. B 56 (1997) 1520.
[33] K. Miwa, A. Fukumoto, Phys. Rev. B 48 (1993) 7897.
[34] L. Filippidis, H. Siegle, A. Hoffmann, C. Thomsen, K. Karch, F. Bechstedt, Phys. Stat. Sol. B 198 (1996) 621.
[35] A.S. Barker Jr., A.J. Sievers, Rev. Mod. Phys. 47 (1975) S1.
[36] C. Wetzel, H. Amano, I. Akasaki, J.W. Ager III, M. Topf, B.K. Meyer, Physica B 273–274 (1999) 109.
[37] R.C. Newman in Imperfections in III/V Materials, Ed. E.R. Weber, p. 144.
[38] C.J. Fall, R. Jones, P.R. Briddon, S. Öberg, Mater. Sci. Eng. B, in press.
[39] J.A. Wolk, W. Walukiewicz, M.L.W. Thewalt, E.E. Haller, Phys. Rev. Lett. 68 (1992) 3619.
[40] B.-C. Chung, M.J. Gershenzon, J. Appl. Phys. 72 (1992) 651.

[41] W.M. Chen, I.A. Buyanova, Mt. Wagner, B. Monemar, J.L. Lindstrom, H. Amano, I. Akasaki, Phys. Rev. B 58 (1998) R13351.
[42] D. Meister, M. Bohm, M. Topf, W. Kriegseis, W. Burkhardt, I. Dirnstorfer, S. Rosel, B. Rosel, B.K. Rosel, A. Hoffmann, H. Siegle, C. Thomsen, J. Thomsen, F. Bertram, J. Appl. Phys. 88 (2000) 1811.
[43] S. Yoshida, S. Misawa, S. Gonda, J. Appl. Phys. 53 (1982) 6844.
[44] M.D. McCluskey, N.M. Johnson, C.G. Van de Walle, D.P. Pour, M. Kneissl, W. Walukiewicz, Phys. Rev. Lett. 80 (1998) 4008.
[45] C. Skierbiszewski, T. Suski, M. Leszczynski, M. Shin, M. Skowronski, M.D. Bremser, R.F. Davis, Appl. Phys. Lett. 74 (1994) 3833.
[46] H. Amano, private communication, 2000.
[47] L.J. Schowalter, Y. Shusterman, R. Wang, I. Bhat, G. Arunmozhi, G.A. Slack, Appl. Phys. Lett. 76 (2000) 985.
[48] R. Zeisel, M.W. Bayerl, S.T.B. Goennenwein, R. Dimitrov, O. Ambacher, M.S. Brandt, M. Stutzmann, Phys. Rev. B 61 (2000) R16283.
[49] P. Boguslawski, E.L. Briggs, J. Bernholc Appl. Phys. Lett. 69 (1996) 233.
[50] P. Boguslawski, J. Bernholc, Phys. Rev. B 56 (1997) 9496.
[51] J. Neugebauer, C.G. Van de Walle, Proceedings of ICPS-22, World Scientific, Singapore 1995, p. 2327.
[52] J.H. Harris, R.A. Youngman, in: J.H. Edgar (Ed.), Properties of Group III Nitrides, INSPEC, IEE, London, UK, 1994, pp. 203–221.
[53] R.A. Youngman, J.H. Harris, J. Am. Ceram. Soc. 73 (1990) 3238.
[54] J. Pastrnak, S. Pacesova, L. Roskocova, Czeck. J. Phys. B 24 (1974) 1149.